AIAA Aerospace Sciences Meeting January 6-9, 2003 Reno, NV AIAA-2003-0179

Characterization of High-Frequency Excitation of a Wake by Simulation©

Alan B. Cain†
Innovative Technology Applications Company
P.O. Box 6971
Chesterfield, MO 63006-6971
ITACabc@aol.com

Michael M. Rogers†
Mail Stop 19-44
NASA Ames Research Center
Moffett Field, CA 94035
mrogers@nas.nasa.gov

Valdis Kibens†
The Boeing Company
MC S111-1240
P.O. Box 516
St. Louis, MO 63166
valdis.kibens@boeing.com

Abstract

Insights into the effects of high-frequency forcing on free shear layer evolution are gained through analysis of several direct numerical simulations. High-frequency forcing of a fully turbulent plane wake results in only a weak transient effect. On the other hand, significant changes in the developed turbulent state may result when high-frequency forcing is applied to a transitional wake. The impacts of varying the characteristics of the high-frequency forcing are examined, particularly the streamwise wavenumber band in which forcing is applied and the initial amplitude of the forcing. The high-frequency excitation is found to increase the dissipation rate of turbulent kinetic energy, to reduce the turbulent kinetic energy production rate, and to reduce the turbulent kinetic energy density for a sustained period after the transition process is complete. The magnitude of the suppression increases with forcing amplitude once a threshold level has been reached. For a given initial forcing energy, the largest reduction in turbulent kinetic energy density was achieved by forcing wavenumbers that are about two to three times the neutral wavenumber determined from linear stability theory.

Introduction

More detailed background for this work has been given in Cain et al. (2001); a brief summary is repeated here to aid the reader. In the early 1990's, Glezer and his co-workers found that forcing at frequencies too high to affect the production scales directly led to a dramatic alteration in the development of a turbulent shear

† Associate Fellow AIAA

layer. An experimental study of this phenomenon was presented by Wiltse and Glezer (1998). Analysis of measurements of jet shear-layer turbulence showed that the direct excitation of small-scale motion by high-frequency forcing led to an increase in the turbulent dissipation rate of more than an order of magnitude in the initial region of the shear layer. High-frequency forcing increased the turbulent kinetic energy in the initial region near the actuators, but the kinetic energy decreased quite rapidly with downstream distance, dropping to levels that were a small fraction of the level for the unforced case. Perhaps most importantly from the present standpoint, high-frequency forcing significantly decreased the energy in the large scale motion, especially with increasing downstream distance.

There are, in fact, earlier hints of such behavior. Examples of relevant earlier work include Vlasov and Ginevskiy (1974), Zaman and Hussain (1981) and Zaman and Rice (1992). These earlier works studied the effect of forcing free shear flows at frequencies roughly 50% higher than the dominant natural frequency. Zaman and Hussain (1981) and Zaman and Rice (1992) found that such forcing reduces the turbulent intensity downstream of the forcing. This result is consistent with the work of Glezer and associates; however, forcing at frequencies 50% greater than the dominant natural frequency still results in the excitation of amplified instabilities of the flow. In fact, these earlier studies attribute the reduced intensities to earlier saturation of the forced instabilities. In Cain et al. (2001), as well as in the work of Glezer, the forcing frequencies are much too high to excite amplified instabilities in the flow. Nonlinear processes are an essential part of the interpretation of the phenomenon, as the results of this study will show.

The initial work of Wiltse and Glezer(1998) has expanded into other applications. Raman, Kibens, Cain, and Lepicovsky (2000) explored the potential of high-frequency forcing for active acoustic suppression. Dramatic results, such as reductions of 20 dB in spectral peaks and 5-8 dB in overall levels across the entire acoustic spectrum, were obtained in some cases. Sample results are presented in Figs. 1 and 2. Similar reductions in noise level were obtained in transonic experiments, as discussion in Raman et al. (2000) and Stanek, Raman, Kibens, and Ross (2000). Other experiments have shown significant potential of high-frequency forcing in controlling reaction rates in chemically reacting flows (see Davis 2000).

The above experiments offer a new set of control concepts that are in sharp contrast to earlier ideas on how control of free shear flows should be approached. The review by Ho and Huerre (1984) characterizes the perspectives of the 1970's and 1980's, demonstrating the link between large-scale structures and linear stability theory. Drazin and Reid (1981) identify approaches to linear stability theory that determine the scale of exponentially growing disturbances. The work by Ho and Huerre (1984) extends the earlier stability theory/large-scale structure ideas by discussing vortex pairing and the more general merging of many large scale structures. Ho and Huerre (1984) provide convincing experimental demonstrations of flow control by excitation frequencies that produce exponentially growing disturbances according to linear stability theory. Cain and Thompson (1986) provide another example of the merits of linear stability analysis. They show that the growth rates predicted by linear theory are able to predict the evolution of finite amplitude disturbances to a saturated state as given by a full nonlinear simulation. These are a few examples of many studies that characterize the control possibilities in free shear flows using ``low-frequency", stability-theory-guided frequency selections. The studies outlined above constitute a major departure from this earlier work. These recent studies do not dispute the results of the earlier work, but challenge the assumption that turbulence theory and linear stability theory preclude interesting effects in the ``high-frequency" excitation regime. Control effects using the new ``high-frequency" excitation regime are currently lacking a theoretical explanation and the present study is aimed at adding detailed quantitative insight into this phenomenon.

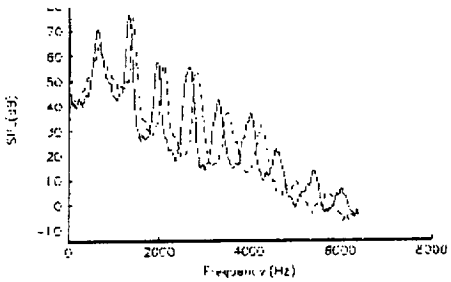

Fig. 1 Effect of high frequency excitation on an edgtone spectrum. Actuator: frequency 5,000Hz, displacement 0.2 μm, Freestream speed M=0.07. Primary edgetone at 672 Hz.
No forcing ———— , with high frequency forcing - - - - - -.

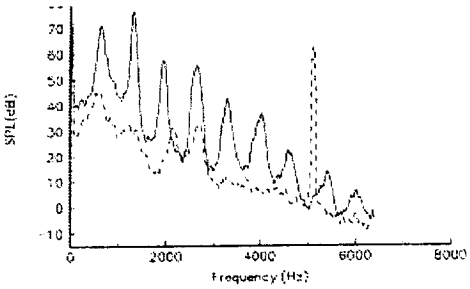

Fig. 2 Effect of high frequency excitation on an edgtone spectrum. Actuator: frequency 5,000Hz, displacement 6.0 μm, M=0.07. Primary edgetone at 672 Hz. No forcing————, with high frequency forcing - - - - - - .

Computational Approach

There is a need to understand the basic mechanism behind effective high-frequency forcing so that scaling laws can be developed to facilitate reliable large-scale system design. Previous experiments sometimes produce dramatic results, but other high-frequency control systems don't show similar improvements. An understanding of the physics is required to ensure reliable application of the technology.

We use direct numerical simulations of free shear layers to investigate the impact of high frequency forcing on various aspects of shear layer evolution. The pseudospectral free shear layer code used by Rogers and Moser (1994) and Moser, Rogers, and Ewing (1998), as modified in Rogers (2002), has been used to simulate incompressible, temporally evolving, plane wakes. To capture the nonlinear physics it has been necessary to use up to 37,000,000 spectral modes in these simulations. Although the temporally evolving flow possesses symmetries not present in spatially developing flows, the dynamics of the large-scale structures are similar in these two flows and the results obtained here should be relevant to spatially developing flows as well. Thus the incompressible flows simulated here should be comparable to the experimental flows of Wiltse and Glezer (1998).

Numerical simulations of high-frequency forcing applied to both fully turbulent and transitional plane wakes have been performed. The self-similar (weakly) forced wake ``fwak" of Moser et al. (1998) has been used as the baseline flow for the fully turbulent cases for reasons outlined in Cain et al. (2001). A single new fully turbulent case ``turb5" has been generated to complement those discussed by Cain et al. (2001). As with the other cases described there, the high-frequency forcing was applied at time $t_f = 12.17$ in the baseline ``fwak" simulation.

Nine additional simulations of high-frequency forcing applied to transitional wakes have also been generated. The baseline flow for these cases ``trans", a transitional flow without high-frequency forcing, is generated by reducing the amplitude of the fluctuating field of ``fwak" at time $t_f = 12.17$ by a factor of ten, leaving the mean flow unaltered. This modified base flow ``trans" has thus been ``relaminarized" to a large extent, but still contains broad band three dimensional disturbances. High-frequency forcing of this transitional flow is applied at the same time $t_f = 12.17$. Further discussion of these baseline flows and the characteristics of the high-frequency forcing used can be found in Appendix A of Cain et al. (2001). The original paper by Moser et al. (1998) may also be of value to those seeking a deeper understanding of the ``fwak" flow and the computational details of these simulations.

Results

In order to verify that the forcing implemented in the computations is qualitatively similar to that used in experiments, energy spectra as a function of the streamwise wavenumber for each of the velocity components have been examined. As shown in Cain et al. (2001), these spectra are similar to those observed by Wiltse and Glezer (1998), with the energy associated with the forcing being at about the same relative wavenumber, of similar relative width in wavespace, and of similar amplitude compared to the energetic large scales of the turbulence. In this work the forcing frequency and amplitude are varied in order to assess how these factors affect the response to high-frequency forcing.

The effects of high-frequency forcing on fully turbulent plane wakes die out quickly and have no lasting impact, as shown by Cain et al. (2001). In order to confirm that this conclusion is still valid for even higher forcing amplitudes, another turbulent case ``turb5" was generated. This case is identical to the ``turb4" case described in Cain et al. (2001), except that f was chosen to be 500 rather 250 (see Table 1 of that work, noting that the non-zero values of α were incorrectly divided by $\left(b^0\right)^2$ and should actually be 9.08). This increase in forcing strength did not have a lasting impact on the flow evolution, reconfirming the insensitivity of turbulent wakes to the high-frequency forcing used here.

As shown in Cain et al. (2001), high-frequency forcing can have a lasting impact on transitional free shear layers. In order to better understand how this impact is dependent on the character of the forcing, nine additional simulations of forced transitional wakes were made. The parameters describing the forcing in these new cases are given in Table 1, along with those from the ``ftrans" case from Cain et al. (2001). Note that in all of these computations only the two lowest spanwise wavenumbers have been forced; this choice was found in Cain et al. (2001) to have the most impact on the wake evolution. Also, in all of the computations, the cross-stream (y) profile of the forcing is given by $a0+f\exp\left\{-\alpha\left(|y|-l\right)^2/b0^2\right\}$, with $a0=1.0$ and off-centerline peaks at $l/b0=0.94$. The three forcing parameters that are varied in these cases are the forcing amplitude f, the range of forced streamwise wavenumbers, and the width of the off-centerline peaks in the forcing y-profile (set by α).

By comparing the ``ftrans" and ``fnarstr" cases, the impact of narrowing the forcing profile in y while maintaining the same total forcing energy can be assessed. Examination of a number of statistics of the type investigated below indicates that the wake development is not sensitive to the choice of α as long as the wavenumber forcing range and total forcing energy are the same. Thus of primary interest here will be investigating the impact of varying these latter two parameters.

As can be seen in Table 1, the simulations ``fhalftr", ``ftrans", and ``fdoubtr" are identical except for the forcing amplitude $f$. Similarly, ``lowq2" and ``lowen" also only differ in the value of $f$ used. These cases can be used to assess the effects of the strength of the forcing, and have been grouped in Table 2 along with ``fnarstr" and the baseline no forcing case ``trans". Table 2 lists several statistics that quantify the impact of the forcing, as discussed later.

Similarly, cases ``ftrans", ``lowq2", ``dlowq2", ``ddlow", ``neutral", and ``best" all have the same initial forcing energy and differ only in the streamwise wavenumber band being forced (with the exception of ``ftrans", which a smaller value of α). These cases have been grouped in Table 3, which includes statistics used to assess the effect of the streamwise wavenumber forcing band. Note that because the forced streamwise wavenumbers are different between these cases, the initial enstrophy varies significantly (by a factor of almost 18) even though the initial forcing energy is the same.

Unlike the insensitivity to the shape of the cross-stream forcing profile, the wake evolution is sensitive to both the forcing amplitude and the streamwise wavenumber band forced. The greatest reductions in turbulence kinetic energy levels from the unforced baseline ``trans" case were obtained for the ``ddlow" and ``best" cases, with the average energy density at a fixed time being the lowest for ``best" case. As will be

discussed later, these flows were forced at lower streamwise wavenumbers than those examined in Cain et al. (2001). In Figs. 3, 4, and 5 the results from the ``ddlow'' case are compared with those of the baseline ``trans'' case to characterize the changes in flow evolution achievable with high-frequency forcing.

Case	$k_x L_x/(2\pi)$	f	α	α/b^0
fhalftr	[129,139]	1250	9.08	0.5
fdoubtr	[129,139]	5000	9.08	0.5
ftrans	[129,139]	2500	9.08	0.5
fnarstr	[129,139]	3572	36.3	2.0
lowq2	[99,109]	2133	36.3	2.0
lowen	[99,109]	2626	36.3	2.0
dlowq2	[69, 79]	926	36.3	2.0
ddlow	[39, 49]	380	36.3	2.0
best	[18, 28]	147	36.3	2.0
neutral	[9, 19]	77.3	36.3	2.0

Table 1

The same initial Turbulent Kinetic Energy (TKE) was set-up for cases fnarstr, lowq2, dlowq2, ddlow, neutral, and best. The same initial enstrophy for cases fnarstr and lowen. The funny values of f were selected to get either the same initial turbulent kinetic energy or enstrophy.

The evolution of the y-integrated turbulent kinetic energy (the flow is homogeneous in the streamwise x and spanwise z directions) is shown in Fig. 3. The turbulence level at t_f is very low in ``trans'', whereas the significant level of high-frequency forcing in ``ddlow'' results in 50 times as much turbulent kinetic energy at t_f. This artificially added energy initially decays, but then grows at a similar, although slightly slower, rate than the disturbance energy in ``trans''. However, the growth of turbulent kinetic energy in ``ddlow'' saturates sooner ($t=280$ instead of $t=500$) and at a lower level (0.133 versus 0.191, or a 30% reduction). High-frequency forcing has apparently resulted in an earlier transition with less intense turbulence once the flow is developed.

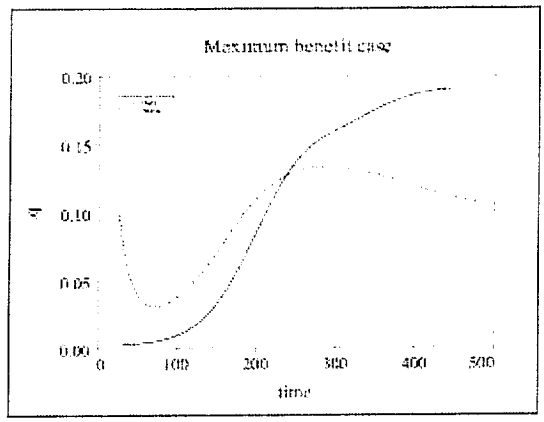

Fig. 3 Cross-stream integrated turbulent kinetic energy as a function of dimensionless time. Transitional initial condition.
Trans base case ————
and high frequency case ddlow - - - - - .

For the time-evolving wakes studied here, the time rate of change of the cross-stream integrated turbulent kinetic energy is equal to the difference between the cross-stream integrated turbulent kinetic energy production rate term and the cross-stream integrated turbulent kinetic energy dissipation rate term. These two integrated quantities are shown in Figs. 4 and 5, respectively, for both the ``ddlow'' and ``trans'' cases.

The changes in the integrated production term with high-frequency forcing are fairly modest. Early in the evolution of the forced ``ddlow'' case this term actually becomes negative, the result of countergradient momentum transport associated with the artificial amplification of the forced modes. This term rapidly becomes positive again, however, and grows at a rate similar to that observed in the unforced ``trans'' case. As with the integrated turbulent kinetic energy, saturation occurs sooner ($t=168$ versus $t=203$) and at a reduced level (0.00126 versus 0.00137, an 8% reduction). The ensuing decay after this saturation is similar, although it occurs about 35 time units sooner for ``ddlow'', consistent with the earlier saturation.

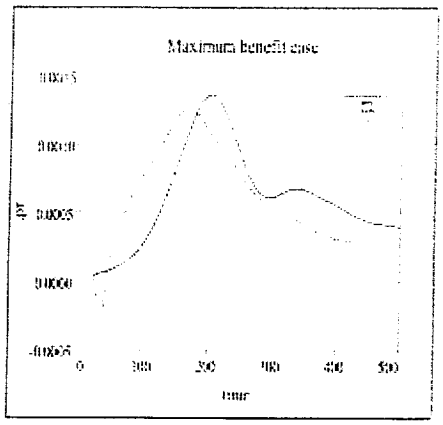

Fig. 4 Cross-stream integrated production rate of turbulent kinetic energy as a function of time. Trans base case ———, and high frequency case ddlow– – – – – .

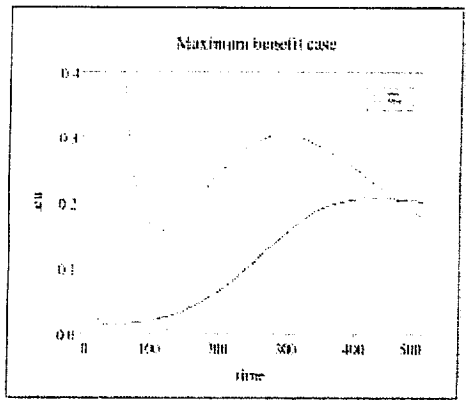

Fig. 5 Cross-stream integrated enstrophy as a function of dimensionless time. Trans base case———, and high- frequency excitation case ddlow– – – – – .

The differences between the integrated dissipation terms for these two cases is much more pronounced (the integrated enstrophy, or dissipation divided by kinematic viscosity of 0.001 is plotted in Fig. 5). Because the forcing energy is applied at high frequencies, the change between the enstrophy/dissipation of the ``ddlow" and ``trans" cases is more marked than that of the turbulent kinetic energy (the initial value being nearly 70 times as large in the forced case). Despite this, the enstrophy decays rapidly initially before increasing at the same rate as in the baseline case. Again, saturation occurs sooner ($t = 289$ versus $t = 438$), but the forced flow saturates at higher enstrophy/dissipation levels than the baseline case (0.301 versus 0.207, a 45% increase).

It is apparent in Fig. 5 that the enstrophy/dissipation level in the forced ``ddlow" case actually drops below that of the baseline case by the end of the simulation. This is not surprising given that the integrated turbulent kinetic energy is greatly reduced at this point (a 45% reduction).

The above results suggest that the primary effect of high-frequency forcing is to modify the way transition occurs in the wake, causing it to occur sooner, with reduced production and enhanced dissipation of turbulent kinetic energy. This in turn leads to an ultimate reduction in flow turbulent kinetic energy once the flow is turbulent, despite the higher initial disturbance levels. In this developed state there is no evidence of a spike in the streamwise wavenumber energy spectra in the forced wavenumber band. The evidence of the forcing is no longer directly apparent but is only reflected in the different character of the resulting turbulence.

Having established that high-frequency forcing can indeed result in reduced turbulent kinetic energy and increased dissipation rate, it is now necessary to see how these changes vary with the forcing amplitude and the streamwise wavenumber of the disturbance. This will in turn permit the development of scaling laws for guidance on how to select these parameters for maximum impact.

First the simulations listed in Table 2 are examined to determine the effect of varying the forcing amplitude at fixed forcing frequency. The evolution of the cross-stream integrated turbulent kinetic energy is shown in Fig. 6 for these cases. Comparisons for two groups of simulations, corresponding to two different streamwise wavenumber bands are considered. One group with forced wavenumbers $k_x L_x/(2\pi)$ between 129 and 139 consists of the ``fhalftr" simulation (dashed line, $f = 1250$, results almost identical to the unforced ``trans" case), the ``ftrans" case (solid line, $f = 2500$), and the ``fdoubtr" flow (dotted line, $f = 5000$). The other group has forced wavenumbers $k_x L_x/(2\pi)$ between 99 and 109

and includes ``lowq2" (chain-dashed line, $f = 2133$) and ``lowen" (chain-dotted line, $f = 2626$). The effects of increasing the forcing amplitude are the same for both of these forcing bands. Although the addition of forcing energy initially increases the turbulent kinetic energy at early times, the saturation level occurs sooner and is reduced such that ultimately the case the most high-wavenumber forcing (``fdoubtr") has the lowest integrated turbulent kinetic energy.

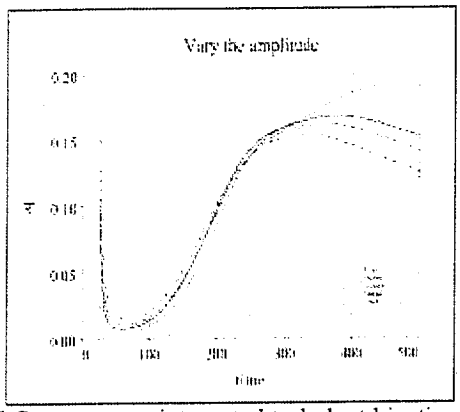

Fig. 6 Cross-stream integrated turbulent kinetic energy as a function of time for cases with varying forcing amplitude.

For the cases shown in Fig. 6 the suppression of turbulence with increasing amplitude is monotonic once a minimum threshold amplitude has been reached. The similarity between the ``trans" and ``fhalftr" cases indicates that the forcing has minimal effect until it reaches a significant amplitude. Beyond this the reduction in energy varies roughly linearly with forcing amplitude, with about the same reduction occurring between ``fhalftr" and ``ftrans" as between ``ftrans" and ``fdoubtr". Of course the suppression must ultimately be limited, but for the amplitudes used here (which are comparable to those used in experiments based on examination of the energy spectra) it appears that further increases in forcing amplitude can still increase the turbulence suppression.

Next the effect of varying the forced streamwise wavenumber band is examined. In Table 3 six forced cases that all have the same initial integrated turbulent kinetic energy and are all forced over a band of 11 computational streamwise wavenumbers are considered. The ``ftrans" and ``lowq2" cases were examined in Fig. 6 and represent cases in which the forcing is occurring at high wavenumbers. As the forcing wavenumbers are reduced (corresponding to forcing larger scales of motion), the physical significance of the forcing changes. For the ``trans" base flow considered here, wavenumbers $k_x L_x/(2\pi)$ of less than about 17 are linearly unstable. For these wavenumbers, infinitesimal disturbances will grow in magnitude (the most unstable streamwise wavenumber being about 6 when scaled this way). The ``best" case, in which wavenumbers between 18 and 28 are forced, is thus not really a ``high-frequency" forced case but is rather a case in which the lowest linearly stable wavenumbers are being forced. The ``neutral" simulation, in which wavenumbers 9 through 19 are forced, includes both linearly unstable and stable modes on either side of the neutral mode. The remaining simulations ``dlowq2" and ``ddlow" are intermediate between these other cases, with forcing of $k_x L_x/(2\pi)$ from 69 to 79 and 39 to 49, respectively.

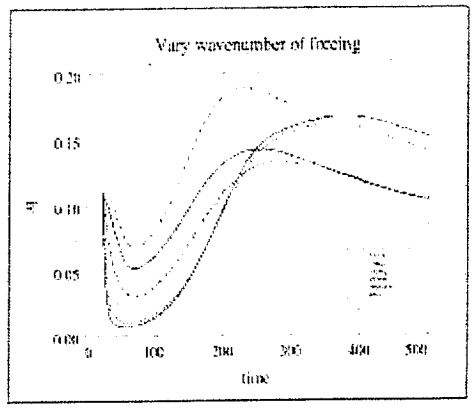

Fig. 7 Cross-stream integrated turbulent kinetic energy as a function of time for cases with different forced streamwise wavenumber bands.

The evolution of the cross-stream integrated turbulent kinetic energy of the six forced flows listed in Table 3 is shown in Fig. 7. As the forcing wavenumbers are decreased in magnitude, the initial turbulent kinetic energy decays more slowly, reaching minima at around $t = 70$ that become progressively larger. As with the results presented in Fig. 6, these higher levels of energy at early times lead to earlier saturation at lower energy levels

and an ultimate suppression of the turbulence. The exception to this trend is the ``neutral" simulation. In this case, growth associated with linearly unstable modes has resulted in overall higher levels of integrated turbulent kinetic energy, of the same order as observed in the unforced ``trans" and weakly forced ``fhalftr" cases. Based on the measure shown in Fig. 7, for which the late-time evolutions of cases ``ddlow" and ``best" are the same, the benefit of continual decrease of the forcing wavenumber is reduced or eliminated before the neutral wavenumber is reached.

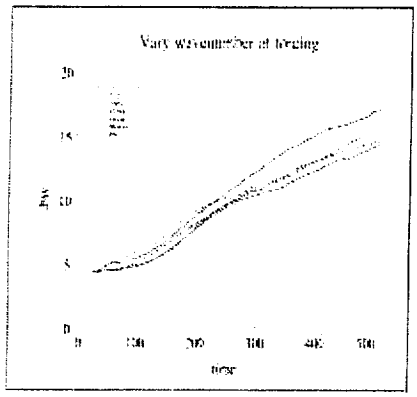

Fig. 8 Wake width as a function of time for cases with different forced streamwise wavenumber bands.

The cross-stream integrated turbulent kinetic energy examined so far is not an energy density; it may vary depending on the wake width as well as on the local turbulence kinetic energy levels. It is thus important to examine the wake width evolution when interpreting this statistic. The evolution of the wake width (here taken as the distance between the points where the mean velocity deficit is half its maximum amplitude) for the forced cases listed in Table 3 is shown in Fig. 8. The evolution for most of the cases is very similar, although the ``neutral" (chain-dotted line) and ``best" (upper solid line) wakes spread somewhat more rapidly, at least early on. At least in the ``neutral" case, this is likely a result of forcing linearly unstable streamwise wavenumbers. The evolutions for the other high-frequency forced cases listed in Table 2 are very similar to those in the lower cluster of curves in Fig. 8. Because the wake spreading rate for the high-frequency forced cases is so similar, conclusions drawn above for the integrated turbulent kinetic energy also generally hold for the turbulent kinetic energy density, although because the wake is spreading in time similar maxima at different times will result in different peak energy densities when normalized by the wake width. From here on the energy density *qden*, the cross-stream integrated turbulent kinetic energy normalized by the wake width, is used to characterize the turbulence levels rather than the integrated energy.

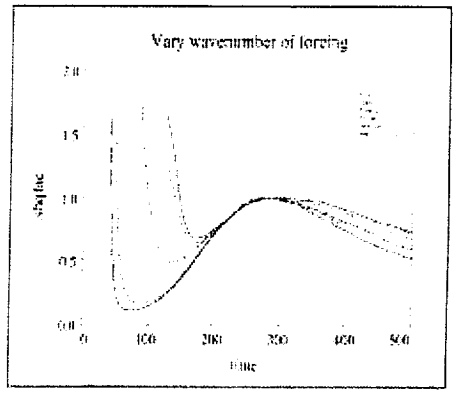

Fig. 9 Normalized turbulent kinetic energy density as a function of shifted time for cases with different forced streamwise wavenumber bands.

The evolutions shown in Fig. 7 are varied, but show the same general trends as each flow develops. By scaling these data it should therefore be possible to extract a more universal response curve. Here a simple scaling is implemented, in which the time axis is shifted (without be compressed or expanded) so that the qden maxima of each of the cases occurs at about 290, close to that of the unforced baseline case. The exact value of the shift selected is fine-tuned to obtain collapse of the various *qden* trajectories prior to this maximum, since this growth is dictated largely by linear theory and should be fairly universal. Additionally, the curves are each scaled by the *qden* maximum to ensure that the peaks of the scaled curves are at the same location. The result of this scaling procedure for the forced cases listed in Table 3 is shown in Fig. 9. The curves for the cases listed in Table 2 are similar. After a rapid initial decay of the artificially added forcing energy, the growth of

the scaled $qden$ does indeed occur at a similar rate among all the cases. The decay after the peak occurs at approximately the same rate, occurring slightly faster as the forcing streamwise wavenumber decreases. The near-universality of the development in Fig. 9 provides further evidence that the main effect of the forcing is to change the timing of the transition process.

The reciprocal of the maximum of the kinetic energy density for each case can be used to characterize the level of turbulence suppression caused by the forcing. This measure is plotted in Fig. 10 for the cases listed in Table 3. All of the forced cases have the same initial integrated turbulent kinetic energy and kinetic energy density as a result of the imposed high-frequency excitation. The maximum suppression occurs for the ``ddlow" case, with forcing between streamwise wavenumbers k_x of 2.45 and 3.08. These wavenumbers are roughly 2.7 times the wavenumber of the neutral mode from linear theory.

In Fig. 11 the measure of turbulence suppression is plotted against the initial integrated turbulent kinetic energy level for the cases listed in Table 2. The two lines represent fits to the data from cases with forcing in two different wavenumber bands. The more extensive data for the cases with forcing $k_x L_x/(2\pi)$ between 129 and 139 suggest a small threshold below which no effect is observed, followed by a region of roughly linear increase with initial turbulent kinetic energy level. The data from the cases with forcing $k_x L_x/(2\pi)$ between 99 and 109 are not as linear and may be showing signs of saturation with continued increase in forcing amplitude.

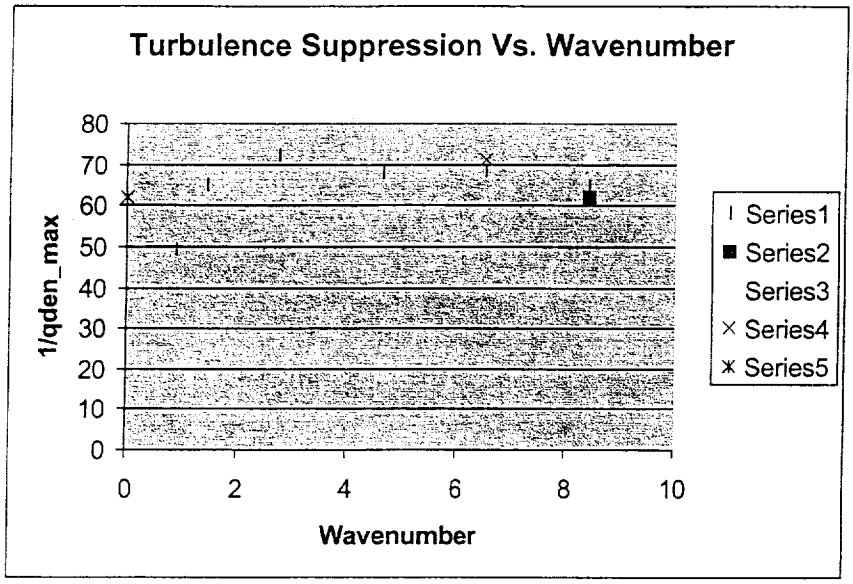

Fig. 10 The measure of turbulence suppression ($1/qden_{\max}$) plotted against the center streamwise wavenumber k_x of the forced wavenumber band for cases with different forced streamwise wavenumber bands.

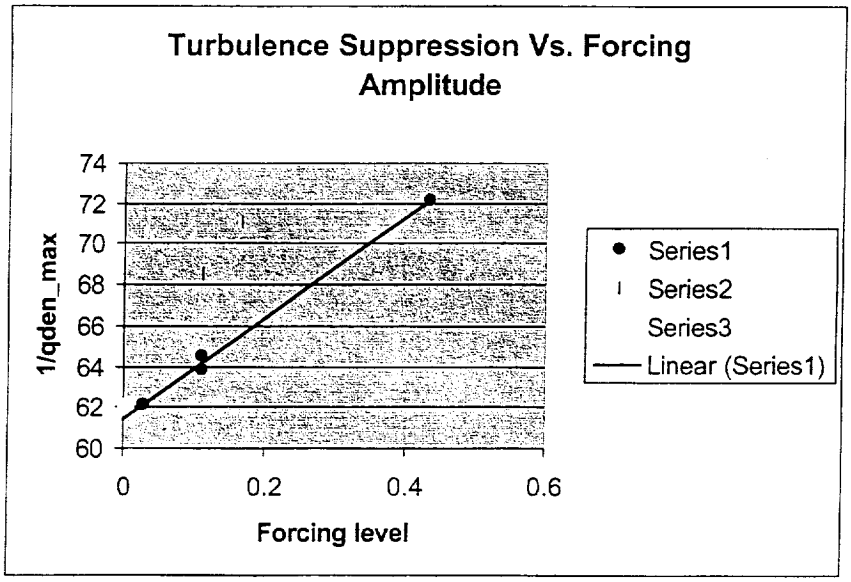

Fig. 11 The measure of turbulence suppression ($1/qden_{\max}$) plotted against the initial integrated turbulent kinetic energy level for cases listed in Table 2. The line represent fits to the data from cases with forcing in one of the wavenumber bands.

Case	$q^2(t_f)$	t_shift	$1/qden\_\max$	k_x_mid
trans	2.23E-3	0	62.1	No forcing
fhalftr	2.88E-2	2.36	62.1	8.42 (134)
fnarstr	1.10E-1	22.9	63.8	8.42 (134)
ftrans	1.10E-1	18.1	64.5	8.42 (134)
fdoubtr	4.33E-1	67.2	72.1	8.42 (134) Max
lowq2	1.10E-1	26.2	68.5	6.53 (104)
lowen	1.66E-1	38.3	71.1	6.53 (104) Max

Table 2
Effect of varying amplitude for a fixed wavenumber.

Case	$q^2(t_f)$	t_shift	$1/qden\_\max$	k_x_mid
trans	2.23E-3	0	62.1	No forcing
neutral	1.10E-1	95.8	49.2	0.88 (14)
best	1.10E-1	100	65.0	1.45 (23)
ddlow	1.10E-1	62.3	72.0	2.76 (44) Max
dlowq2	1.10E-1	45.1	68.0	4.65 (74)
lowq2	1.10E-1	26.2	68.5	6.53 (104)
ftrans	1.10E-1	18.1	64.5	8.42 (134)

Table 3
Parameters for the cases of varying wavenumber at fixed amplitude.

Conclusions

Unlike fully turbulent wakes, which are largely insensitive to high-frequency forcing, transitional wakes subjected to high-amplitude high-frequency forcing do evolve to different turbulent states. Direct numerical simulations have been used to determine how high-frequency forcing effects the resulting developed turbulent flow. High-frequency forcing is found to increase the turbulent kinetic energy dissipation rate, reduce the turbulent energy production rate, and reduce the level of turbulent kinetic energy for a sustained period after the transition process is complete. Both the band of streamwise wavenumbers forced and the amplitude of the forcing have been systematically varied to ascertain which values of these parameters result in maximum turbulence suppression. This suppression is found to increase monotonically over the forcing amplitude range examined, although there is apparently a minimum threshold amplitude required to achieve an effect. The optimal forcing wavenumbers found here are relatively smaller than those used in most experiments involving high-frequency forcing. For a fixed amount of forcing energy, the greatest suppression of turbulent kinetic energy density was achieved when the forced wavenumbers were 2 to 3 times the wavenumber of the neutrally stable disturbance from linear theory.

Acknowledgements

This work was motivated by the Boeing/DARPA HIFEX Program and first author wishes to acknowledge support from the Boeing/DARPA HIFEX Program during the execution of this work. This work benefited from discussions with Prof. A. Glezer regarding related experimental work and also from the high quality Boeing/DARPA program management by Dr. W. Bower.

References

1. Cain, A. B., Rogers, M. M., Kibens, V., and Raman, G., "Simulations of High-Frequency Excitation of a Plane Wake," AIAA-2001-0514, Presented at the AIAA Aerospace Sciences Meeting, Reno, NV, Jan., 2001.

2. Wiltse, J.M. & Glezer, A., 1998, "Direct excitation of small-scale motions in free shear flows," Phys. Fluids, vol. 10, pp. 2026--2036.

3. Vlasov, Y.V. and Ginevskiy, A.S., 1974, "Generation and Suppression of Turbulence in an Axisymmetric Turbulent Jet in the Presence of an Acoustic Influence," NASA TT-F-15, 721, 1974.

4. Zaman, K.B.M.Q. and Hussain, A.K.M.F., 1981, "Turbulence Suppression in Free Shear Flows by Controlled Excitation," J. Fluid Mech. Vol. 103, pp. 133-159.

5. Zaman, K.B.M.Q. and Rice, E.J., 1992, "On the Mechanism of Turbulence Suppression in Free Shear Flows Under Acoustic Excitation," AIAA-92-0065, Presented at the 30th Aerospace Sciences Meeting.

6. Raman, G., Kibens, V., Cain, A. & Lepicovsky, J., 2000 "Advanced actuator concepts for active aeroacoustic control." AIAA 2000-1930, 6th AIAA/CEAS Aeroacoustics Conference, June 2000, Lahaina, Hawaii.

7. Stanek, M., Raman, G., Kibens, V. and Ross, J., 2000, "Cavity tone suppression using high frequency excitation," AIAA 2000-1905, 6th AIAA/CEAS Aeroacoustics Conference, June 2000, Lahaina, Hawaii.

8. Davis, S. A., 2000, "The manipulation of large and small flow structures in single and coaxial jets using synthetic jet actuators," Ph.D. thesis, Georgia Institute of Technology, May 2000.

9. Ho, C. M., Huerre, P., 1984, "Perturbed Free Shear layers," Annual Review of Fluid Mechanics, vol. 16, p. 365.

10. Drazin P.G. & Reid, W.H., 1981, "Hydrodynamic Stability," Cambridge University Press.

11. Cain, A. B. & Thompson, M. W., 1986, "Linear and Weakly Nonlinear Aspects of Free Shear Layer Instability, Roll-Up, Subharmonic Interaction and Wall Influence," AIAA-86-1047, May, 1986.

12. Rogers, M. M. & Moser, R. D., 1994, "Direct simulation of a self-similar turbulent mixing layer," Phys. Fluids vol. 6, pp. 903--923.

13. Moser, R. D., Rogers, M. M. & Ewing, D. W., 1998 "Self-similarity of time-evolving plane wakes," vol. 367, pp. 255--289.

14. Rogers, M. M., 2002, "The evolution of strained turbulent plane wakes," J. Fluid Mech., Vol. 463, pp. 53-120.